ULTRASONIC IMAGING 4, 336-350 (1982)

# A FILTERED BACKPROPAGATION ALGORITHM FOR DIFFRACTION TOMOGRAPHY

A. J. Devaney

Schlumberger-Doll Research
P. O. Box 307
Ridgefield, CT 06877

A reconstruction algorithm is derived for parallel beam transmission computed tomography through two-dimensional structures in which diffraction of the insonifying beam must be taken into account. The algorithm is found to be completely analogous to the filtered backprojection algorithm of conventional transmission tomography with the exception that the backprojection operation has to be replaced by a back*propagation* process whereby the complex phase of a field measured over a line outside the object is made to *propagate* back through the object space. The algorithm is applicable to diffraction tomography within either the first Born or Rytov approximations. Application of the algorithm to three-dimensional structures is also discussed.

Key words: Backprojection; image reconstruction; inverse scattering.

## 1. INTRODUCTION

In conventional parallel beam transmission computed tomography one reconstructs an object profile $O(x,y)$ representing, for example, an x-ray attenuation coefficient, from the object's projections

$$P_\phi(\xi) = \int O(x,y)\, d\eta \quad , \tag{1}$$

where $(\xi,\eta)$ denote the coordinates in a cartesian coordinate system rotated by the angle $\phi$ relative to the $(x,y)$ system (Fig. 1a). The reconstruction of $O(x,y)$ from $P_\phi(\xi)$ is made possible by the *projection-slice theorem* [1] which states that the one-dimensional Fourier transform of $P_\phi(\xi)$ is a *slice* at angle $\phi$ through the two-dimensional Fourier transform of $O(x,y)$ (Fig. 1b). The projections $P_\phi(\xi)$ then yield, upon Fourier transformation, an ensemble of slices of the two-dimensional Fourier transform $\tilde{O}(K_x,K_y)$ of $O(x,y)$ . $O(x,y)$ can then readily be reconstructed from this ensemble of slices via its Fourier integral representation expressed in circular polar coordinates. In particular, one finds that [1,2]

$$O(x,y) \approx \frac{1}{(2\pi)^2}\int_0^\pi d\phi \int_{-W}^{W} dK\, |K|\, \tilde{P}_\phi(K) e^{iK[x\cos\phi + y\sin\phi]} \quad , \tag{2}$$

where

$$\tilde{P}_\phi(K) = \int_{-\infty}^{\infty} d\xi P_\phi(\xi) e^{-iK\xi} \tag{3}$$

is the one-dimensional Fourier transform of $P_\phi(\xi)$ . In Eq. (2) we have limited the K integration interval to -W to W since, in any application, $\tilde{P}_\phi(K)$ will be known only over a finite bandwidth which we have taken to be -W to W . Because of this the resulting reconstruction is only approximate being, in fact, a low pass filtered version of $O(x,y)$ .

In practice one uses in place of the Fourier integral representation, Eq. (2), the so-called *filtered backprojection algorithm* to reconstruct $O(x,y)$ [2] . Defining the filter function

$$h(t) \equiv \frac{1}{2\pi}\int_{-W}^{W} dK\, |K|\, e^{iKt}$$

$$= \frac{1}{\pi}W^2[\sin(KW)/(KW)] - \frac{1}{2\pi}W^2[\sin(KW/2)/(KW/2)]^2 \quad , \tag{4}$$

it is easily shown [2] that Eq. (2) can be written in the form

$$O(x,y) \approx \frac{1}{2\pi}\int_0^\pi d\phi\; Q_\phi(x\cos\phi + y\sin\phi) \quad , \tag{5}$$

where $Q_\phi(t)$ , called *filtered projections* , are given by

$$Q_\phi(t) = \int_{-\infty}^{\infty} P_\phi(\xi) h(t-\xi) d\xi \quad . \tag{6}$$

0161-7346/82/040336-15$02.00/0

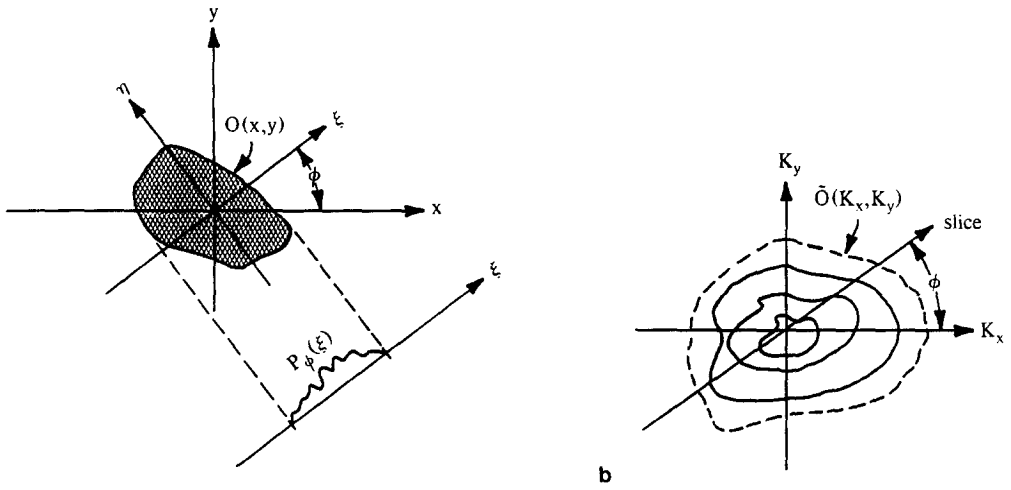


Fig. 1 (a) Coordinate systems and associated geometry for defining line projections $P_\phi(\xi)$ of two-dimensional profiles O(x,y). (b) One-dimensional Fourier transform of $P_\phi(\xi)$ yields two- dimensional transform $\tilde{O}(K_x, K_y)$ along the line (slice) passing through the origin and making the angle $\phi$ with the positive $K_x$ axis.

The process of reconstructing O(x,y) consists then of first *filtering* the projections with the filter function h(t) and then *backprojecting* the filtered projections according to Eq. (5). In practice, of course, the filtered projections will only be known for a finite number of angles so that a discrete approximation to the backprojection integral Eq. (5) must be employed [2].

The success of transmission computed tomography clearly depends on the availability of the projections $P_\phi(\xi)$ . In x-ray tomography these projections are available in the form of measurements of the log amplitude [1/2 log(intensity)] of the electromagnetic field produced when a plane, monochromatic x-ray beam propagating along the $\eta$ axis is incident to the object as is illustrated in figure 2. At x-ray wavelengths ( $\approx 1\text{Å}$ ) the incident plane wave suffers essentially no scattering (refraction or diffraction) in passing through the object. Absorbtion does occur, however, so that the negative of the log amplitude of the field along the line $\eta=l_0$ is simply the integrated value of the x-ray absorbtion coefficient $\mu(x,y)$ along the travel path ( i.e., along the straight line $\xi$=constant ). The object profile O(x,y) in this case is then $\mu(x,y)$ and the projections $P_\phi(\xi)$ are simply the negative of the log amplitude of the electromagnetic field as measured along the line $\eta=l_0$ .

In ultrasonic tomography the wavelength is considerably greater ($\approx$1m.m.) than that of x-rays so that an acoustic wave experiences scattering, in the form of refraction and diffraction, in the process of propagating through an object such as biological tissue. The log amplitude of the acoustic field along the line $\eta=l_0$ resulting from an insonifying plane wave propagating along the $\eta$ axis is then not simply the projection of the acoustic absorbtion coefficient along the line $\xi$=constant as is the case in x-ray tomography. This breakdown in the relationship between measured log amplitude and projections of the absorbtion coefficient is one of the major reasons why conventional computed tomography is of limited use in ultrasonic applications [3,4].

Although it is not possible, in general, to obtain an exact, closed form expression for the acoustic field generated by the interaction of an insonifying plane wave with an acoustic profile O(x,y), expressions within the so-called first Born and Rytov approximations are available. Within these approximations one finds [4-6] that for an incident monochromatic plane wave propagating along the $\eta$ axis, the profile O(x,y) is related to the data $D_{\phi_0}(\xi, \omega)$ taken along the line $\eta=l_0$ via the equation

$$\int_{-\infty}^{\infty} d\xi D_{\phi_0}(\xi, \omega)\exp(-i\kappa\xi) = \iint dx\,dy\; O(x,y)\exp(-i[\kappa\xi+(\sqrt{k^2-\kappa^2}-k)\eta]) \quad , \tag{7}$$

where the variable $\kappa$ can assume all values in the range [-k,k]. Here $\phi_0 = \phi + \pi/2$ is the angle that the wavevector of the insonifying plane wave makes with the x axis and $\omega$ is the angular frequency

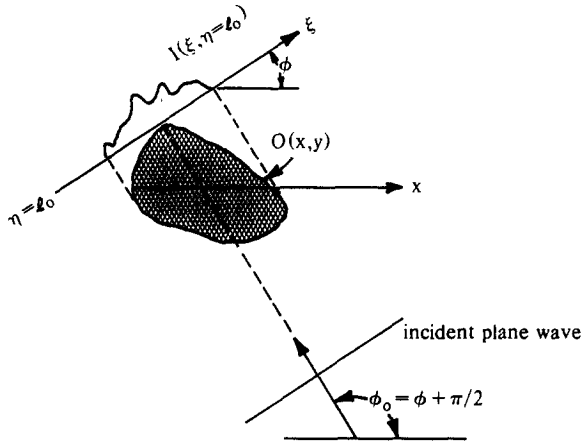


Fig. 2 The log of the intensity $I(\xi,\eta=l_o)$ of the x-ray field over the line $\eta = l_o$ is proportional to the projection $P_\phi(\xi)$ of the object profile.

and $k=2\pi/\lambda$ is the wavenumber of the insonifying acoustic field. The data $D_{\phi_o}(\xi,\omega)$ is, in the case of the Born approximation, simply related to the complex amplitude of the scattered field portion of the acoustic field evaluated along the line $\eta=l_o$ [4,5] and, in the case of the Rytov approximation, to the difference in the complex phase of the total field and incident field evaluated along this same line [4,6]. Which approximate model is selected (Born or Rytov) depends on a number of factors although at very high wavenumbers the Rytov approximation is generally superior [4,6].

It is convenient at this point to introduce the two unit vectors

$$\underline{s} = 1/k(\kappa\,\hat{\underline{\xi}}+\sqrt{k^2-\kappa^2}\,\hat{\underline{\eta}}) \tag{8a}$$

and

$$\underline{s}_o = \hat{\underline{\eta}} \ , \tag{8b}$$

where $\hat{\underline{\xi}}$ and $\hat{\underline{\eta}}$ are unit vectors along the $\xi,\eta$ axes. We note that the unit vector $\underline{s}_o$ is simply the unit propagation vector of the insonifying plane wave. For values of $|\kappa| \leq k$ we find that Eq. (7) can be expressed in terms of $\underline{s}$ and $\underline{s}_o$ in the form

$$\tilde{D}_{\phi_o}(\kappa,\omega) \equiv \int_{-\infty}^{\infty} d\xi D_{\phi_o}(\xi,\omega)e^{-i\kappa\xi} = \int\int dxdy\ O(x,y)e^{-ik(\underline{s}-\underline{s}_o)\cdot\underline{r}} \ . \tag{9}$$

We conclude from Eq. (9) that the one-dimensional Fourier transform $\tilde{D}_{\phi_o}(\kappa,\omega)$ of $D_{\phi_o}(\xi,\omega)$ is equal to the two-dimensional Fourier transform $\tilde{O}(K_x,K_y)$ of the profile $O(x,y)$ evaluated over the locus of points defined by

$$\underline{K} \equiv K_x\hat{\underline{x}}+K_y\hat{\underline{y}}=k(\underline{s}-\underline{s}_o) \ , \tag{10}$$

where the unit vector $\underline{s}$ assumes all values for which $\underline{s}\cdot\underline{s}_o>0$ . The $\underline{K}$ values satisfying Eq. (10) for fixed $\underline{s}_o$ with $\underline{s}\cdot\underline{s}_o>0$ , are seen to lie on a semicircle, centered at $-k\underline{s}_o$ and having a radius equal to k . By changing the direction of propagation of the insonifying plane wave it is thus possible to sample $\tilde{O}(K_x,K_y)$ over an ensemble of semicircular arcs such as illustrated in figure 3. The ultrasonic tomographic reconstruction problem then consists of estimating $O(x,y)$ from specification of $\tilde{O}(K_x,K_y)$ over this ensemble of arcs.

The problem of reconstructing an object profile from specification of its Fourier transform over an ensemble of circular arcs such as shown in figure 3 is an old one having first occurred in x-ray crystallography [7], and later in inverse scattering applications using both x-rays [8] and visible light [9]. More recently, these inverse scattering methods have been applied in ultrasonics [4,5,10] with particular emphasis placed on ultrasonic tomography which has become known as *diffraction tomography* [10] to distinguish it from conventional tomography where diffraction effects are not taken into account. In all of these applications the reconstruction of the profile $O(x,y)$ is made possible by the fact that by varying $\underline{s}_o$ over the unit circle, one can determine $\tilde{O}(K_x,K_y)$ at any point

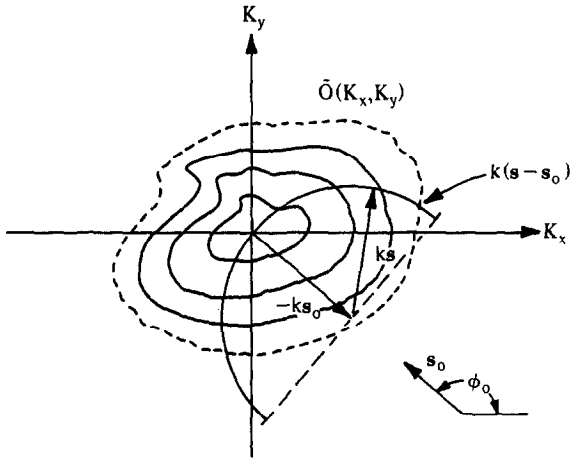


Fig. 3 $\tilde{D}_{\phi_o}(K, \omega)$ equals $\tilde{O}(K_x,K_y)$ evaluated on the semicircle $\underline{K} = k(\underline{s} - \underline{s}_o)$ with $\underline{s}\cdot\underline{s}_o > 0$. Note that in the short wavelength limit $(k \rightarrow \infty)$, this semicircle degenerates into the slice illustrated in figure 1b.

lying within a circle, centered at the origin and having a radius equal to $\sqrt{2}k$. A *low pass filtered version* $O_{LP}(x,y)$ of $O(x,y)$ can then be obtained by means of the Fourier integral representation

$$O_{LP}(\underline{r}) = \frac{1}{(2\pi)^2}\int_{|\underline{K}|\leq\sqrt{2}k} d^2K\, \tilde{O}(\underline{K})e^{i\underline{K}\cdot\underline{r}} \quad , \tag{11}$$

where we have used vector notation so that $\underline{r}=(x,y)$ , $\underline{K}=(K_x,K_y)$ and $d^2K$ stands for the differential surface element in $\underline{K}$ space .

In any application the profile $O(\underline{r})$ will vanish beyond some finite range so that a Fourier series expansion for $O_{LP}(\underline{r})$ can be used in place of the Fourier integral Eq. (11). In the Fourier series expansion the transform $\tilde{O}(\underline{K})$ must then be known for $\underline{K}$ values lying on a regular, square sampling grid in $\underline{K}$ space . To obtain the requisite sample values then requires that either one interpolate $\tilde{O}(K_x,K_y)$ from the sample values given on arcs over which this quantity is known or, alternatively, that one select propagation directions $\underline{s}_o$ such that at least one arc falls on every required sample point in the array. Discussion and examples of the first (interpolation) method can be found in [11] and [12] while the second procedure is followed in [13] and [14].

Both the interpolation and direct sampling methods for obtaining sample values of $\tilde{O}(\underline{K})$ over a regular square sampling grid have serious drawbacks. Interpolation of $\tilde{O}(\underline{K})$ from sample values given on semicircular arcs suffers from the same limitations as does interpolation from slices in $\underline{K}$ space. Reconstructions based on the two-dimensional FFT from interpolated sample values in conventional tomography are well known to be inferior [15] to those obtained via filtered backprojection. Direct sampling methods are undesirable because they generally require a very large number of $\underline{s}_o$ values ( i.e., many experiments ). In addition, both procedures place severe demands on the experimentalist in that they require extreme accuracy in registering data collected from different experiments [11], [14].

In this paper we derive a reconstruction algorithm for diffraction tomography that allows $O_{LP}(\underline{r})$ to be reconstructed directly from $D_{\phi_o}(\xi,\omega)$ without the necessity of first determining $\tilde{O}(\underline{K})$ over a regular square sampling grid in $\underline{K}$ space. The algorithm, called the *filtered backpropagation algorithm*, is completely analogous to the filtered backprojection algorithm of conventional transmission tomography. The two algorithms differ in only one important respect: the backprojection process by which the filtered projections $Q_\phi(t)$ are continued back through the object space along parallel straight line paths in conventional tomography has to be replaced by a process of *backpropagation*. In backpropagation quantities $\hat{Q}_{\phi_o}(t)$, related to the data $D_{\phi_o}(\xi,\omega)$ through the filtering operation (6), are mapped onto the object space via an integral transform that is shown to be the inverse of the transform that governs phase propagation within the Rytov approximation. It is natural then to call this process *backpropagation* since it corresponds mathematically to the inverse of the usual forward

propagation process. The reconstruction algorithm is then called the filtered backpropagation algorithm to emphasize its formal similarity to the filtered backprojection algorithm of conventional tomography.

In Section 2 we review the formulation of diffraction transmission tomography within the first Born and Rytov approximations. We address explicitly *ultrasonic* transmission tomography in two-dimensional biological media although the analysis can readily be extended to three dimensions and to other applications utilizing electromagnetic radiation or particle beams.

The filtered backpropagation algorithm is derived and discussed in Section 3. In Section 4 we discuss the application of the algorithm to three-dimensional structures. It is shown that any desired planar projection of such structures can be reconstructed from application of the algorithm. Moreover, the complete three-dimensional profile can be obtained from an ensemble of these projections by making use of the projection-slice theorem [1]. Section 5 summarizes the results presented in the paper and discusses generalizations and future directions for this work.

## 2. DIFFRACTION TOMOGRAPHY

In this section we shall review briefly the formulation of *diffraction tomography* within the first Born and Rytov approximations. Our principle result will be a derivation of Eq. (9) which forms the basis for most of the results presented in the remainder of the paper.

We consider a two-dimensional object immersed in a fluid medium and insonified with an ultrasonic plane wave pulse $P_o(\underline{r}, t)$ whose unit propagation vector $\underline{s}_o$ lies in the plane of the object. We shall assume that the object has a constant density and a vanishing shear modulus. Both of these assumptions are approximately fulfilled in biological applications [4, 16]. The interaction of the object with the acoustic field is then characterized by the time independent Schrodinger equation

$$( \nabla^2+k^2 )U(\underline{r},\omega) = k^2O(\underline{r})U(\underline{r},\omega) \quad , \tag{12}$$

where $k=\omega/C_o$ is the wavenumber at angular frequency $\omega$ of the acoustic field in the fluid medium with $C_o$ being the compressional wave velocity in the fluid . Here, $U(\underline{r},\omega)$ denotes the ( generally complex) amplitude of a time-harmonic component of the time varying pressure field $P(\underline{r}, t)$ induced by the insonifying pulse $P_o(\underline{r}, t)$ ; i.e.,

$$P(\underline{r}, t) = \frac{1}{2\pi}\int_0^\infty d\omega U(\underline{r},\omega)e^{-i\omega t} + \text{c.c.} \quad , \tag{13}$$

where c.c. stands for the complex conjugate.

The acoustic profile $O(\underline{r})$ is related to the object's compressional wave velocity $C(\underline{r})$ via the equation [4]

$$O(\underline{r}) = 1-C_o^2/C^2(\underline{r}) \quad . \tag{14}$$

Although both the fluid medium velocity $C_o$ and the object velocity $C(\underline{r})$ can exhibit *dispersion* , i.e., depend explicitly on frequency, we shall assume that these quantities are frequency independent which is usually true over broad frequency ranges for biological specimens. However, the analysis and final results remain the same regardless of whether or not this assumption holds true. In addition to dispersion, absorbtion in the form of heat and scattering losses may be present so that $C(\underline{r})$ and, hence, $O(\underline{r})$ will generally be complex.

It is convenient to convert Eq. (12) into an integral equation that incorporates the boundary condition that the time dependent field $P(\underline{r}, t)$ equal the incident field $P_o(\underline{r}, t)$ for times t prior to the interaction of the incident field with the object (causality). One then finds that [17]

$$U(\underline{r},\omega) = U_o(\omega)e^{ik\,\underline{s}_o\cdot\underline{r}} - i\frac{k^2}{4}\int d^2r'\, O(\underline{r}')U(\underline{r}',\omega)H_o(k\,|\underline{r}-\underline{r}'|) \quad , \tag{15}$$

where $H_o(kR)$ is the zero order Hankel function of the first kind and where $U_o(\omega)\exp(ik\,\underline{s}_o\cdot\underline{r})$ is the Fourier amplitude, at frequency $\omega$ , of the insonifying plane wave pulse; i.e.,

$$P_o(\underline{r}, t) = \frac{1}{2\pi}\int_0^\infty d\omega U_o(\omega)e^{ik\,\underline{s}_o\cdot\underline{r}}e^{-i\omega t} + \text{c.c.} \quad . \tag{16}$$

As mentioned in the introduction, it is not possible, in general, to solve exactly for the total pressure field $U(\underline{r},\omega)$ . Two approximate solutions that have been found useful in inverse scattering and diffraction tomography are the first Born approximation and the Rytov approximation. The first

Born approximation is obtained by simply substituting the incident field $U_o(\omega)\exp(ik\,\underline{s}_o\cdot\underline{r}')$ for $U(\underline{r}',\omega)$ in the integral in Eq. (15). One then obtains

$$U(\underline{r},\omega) \simeq U_o(\omega)e^{ik\,\underline{s}_o\cdot\underline{r}} + U_B^{(s)}(\underline{r},\omega) \quad , \tag{17}$$

where

$$U_B^{(s)}(\underline{r},\omega) = -i\frac{k^2}{4}U_o(\omega)\int d^2r'\, O(\underline{r}')e^{ik\,\underline{s}_o\cdot\underline{r}'}\, H_o(k\,|\underline{r}-\underline{r}'|) \tag{18}$$

is the scattered field within the first Born approximation.

The Rytov approximation is not derived from Eq. (15) but rather from a linearized version of the Riccati differential equation satisfied by the complex *phase* $\Psi(\underline{r},\omega)$ of the total pressure field $U(\underline{r},\omega) \equiv \exp\Psi(\underline{r},\omega)$ . The derivation of the complex phase within this approximation is not particularly instructive within the present context and, consequently, will not be presented here. ( The interested reader is referred to the excellent accounts of this approximation presented in [18] and [19] ). One finds that

$$\Psi(\underline{r},\omega) \simeq \Psi_R(\underline{r},\omega) \equiv ik\underline{s}_o\cdot\underline{r} + e^{-ik\underline{s}_o\cdot\underline{r}}\, U_B^{(s)}(\underline{r},\omega) \quad , \tag{19}$$

where $\Psi_R(\underline{r},\omega)$ stands for the Rytov approximation to $\Psi(\underline{r},\omega)$ . *The complex phase* $\Psi(\underline{r},\omega)$ *within the Rytov approximation is thus found to be simply related to the first Born approximation to the scattered field* $U_B^{(s)}(\underline{r},\omega)$ . Although these two approximations are trivially related it is important to point out that the limits of validity of the two approximations are quite different. A discussion of these differences will not be presented here, but can be found in [4] and [6].

Let us take the direction of propagation of the incident plane wave to be along the y axis and assume that the profile $O(\underline{r}')$ vanishes outside a circle centered at the origin and with a radius equal to $l_o$ . We then find that along the line $y=l_o$ the Born approximation to the scattered field $U_B^{(s)}(\underline{r},\omega)$ can be written in the form

$$U_B^{(s)}(\underline{r},\omega) = -i\frac{k^2}{4\pi}U_o(\omega)\int_{-\infty}^{\infty}\frac{dK_x}{\gamma}e^{i\gamma\, l_o}\,\tilde{O}(K_x,\gamma-k)e^{iK_x x} \quad , \tag{20}$$

where $\gamma=\sqrt{k^2-K_x^2}$ and where

$$\tilde{O}(K_x,\gamma-k) = \int\int dxdy\; O(x,y)e^{-i[K_x x + (\gamma-k)y]} \tag{21}$$

is, for values of $|K_x|\leq k$ (real $\gamma$ ), simply the two-dimensional Fourier transform of $O(\underline{r})$ evaluated at $K_y=\gamma-k$ . In deriving Eq. (20) we have made use of the following integral representation of the Hankel function [20]:

$$H_o(k\,|\underline{r}-\underline{r}'|) = 1/\pi\int_{-\infty}^{\infty}\frac{dK_x}{\gamma}e^{i[K_x(x-x')+\gamma\,|y-y'|]} \tag{22}$$

Making use of Eq. (20) we obtain the following expression for the one-dimensional Fourier transform of $U_B^{(s)}(\underline{r},\omega)$ along the line $y=l_o$:

$$\int_{-\infty}^{\infty}dx\; U_B^{(s)}(x,y=l_o,\omega)e^{-i\kappa x} = -i\frac{k^2}{2}U_o(\omega)\frac{e^{i\gamma l_o}}{\gamma}\tilde{O}(\kappa,\gamma-k) \quad , \tag{23}$$

with $\gamma=\sqrt{k^2-\kappa^2}$ . The one-dimensional Fourier transform of the Rytov approximation to the complex phase difference

$$\psi_R(\underline{r},\omega) \equiv \Psi_R(\underline{r},\omega) - ik\underline{s}_o\cdot\underline{r} \tag{24}$$

between the total and incident fields along the line $y = l_o$ is immediately found from Eqs.(19)-(24) to be

$$\int_{-\infty}^{\infty}dx\;\psi_R(x,y=l_o,\omega)e^{-i\kappa x} = -i\frac{k^2}{2}U_o(\omega)\frac{e^{i(\gamma-k)l_o}}{\gamma}\tilde{O}(\kappa,\gamma-k) \quad . \tag{25}$$

Eqs.(23) and (25) can be expressed in the unified form

$$\int_{-\infty}^{\infty}dx\; D(x,\omega)e^{-i\kappa x} = \int\int dxdy\; O(x,y)e^{-i[\kappa x+(\sqrt{k^2-\kappa^2}-k)y]} \quad , \tag{26}$$

where

$$D(x,\omega) = \frac{2i\gamma}{k^2U_o(\omega)}e^{-i\gamma l_o}\, U_B^{(s)}(x,y=l_o,\omega) \tag{27a}$$

or

$$D(x,\omega) = \frac{2i\gamma}{k^2 U_o(\omega)} e^{-i(\gamma-k)l_o} \psi_R(x,y=l_o,\omega) \tag{27b}$$

depending on whether the first Born approximation or Rytov approximation is employed. Although $D(x,\omega)$ depends on $\gamma$ and, hence on $\kappa$ , we shall not explicitly display this dependence in the argument of this quantity.

Eq. (26) is seen to be of the form of Eq. (7) with $\phi_o = \pi/2$ . Indeed, it is not difficult to extend the analysis presented above to the case of an insonifying plane wave propagating along an arbitrary $\eta$ axis such as illustrated in figure 2. One then finds that Eq. (26) generalizes to Eq. (7) with $D_{\phi_o}(\xi,\omega)$ given by

$$D_{\phi_o}(\xi,\omega) = \frac{2\gamma}{k} e^{-i(\gamma-k)l_o} \Gamma_{\phi_o}(\xi,\omega) \quad , \tag{28}$$

where

$$\Gamma_{\phi_o}(\xi,\omega) = \begin{cases} \dfrac{ie^{-ikl_o}}{kU_o(\omega)} U^{(s)}{}_{\phi_o}(\xi,\eta=l_o,\omega) & \text{Born Approximation} \quad (29a) \\ \dfrac{i}{kU_o(\omega)} \psi_{\phi_o}(\xi,\eta=l_o,\omega) & \text{Rytov Approximation.} \quad (29b) \end{cases}$$

In these equations we have dropped the subscripts B and R from $U^{(s)}$ and $\psi$ since these quantities are to be here interpreted as *measured data*. We have added the subscript $\phi_o$ to these quantities to indicate that they depend on the angle $\phi_o$ that the unit propagation vector $\underline{s}_o$ makes with the positive x axis. By introducing the unit vectors $\underline{s}$ and $\underline{s}_o$ according to Eq. (8) our final result can be expressed in the form given in Eq. (9) with $D_{\phi_o}(\xi,\omega)$ given by Eq. (28).

Finally, let us consider diffraction tomography in the limit of vanishing wavelength ($\lambda \to 0$). In this limit we have $\gamma \to k$ so that

$$D_{\phi_o}(\xi,\omega) \to 2\Gamma_{\phi_o}(\xi,\omega) = \frac{2i}{kU_o(\omega)} \psi_{\phi_o}(\xi,\eta=l_o,\omega)$$

within the Rytov approximation. Here, we shall consider only the Rytov approximation since this approximation is known to be superior to the Born approximation in the short wavelength case. Eq. (7) then yields for $\lambda \to 0$

$$\frac{2i}{kU_o(\omega)} \int_{-\infty}^{\infty} d\xi \; \psi_{\phi_o}(\xi,\eta=l_o,\omega) e^{-i\kappa\xi} = \iint dx dy O(x,y) e^{-i\kappa\xi} \quad ,$$

from which it follows from the central-slice theorem [1] that $\frac{2i}{kU_o(\omega)} \psi_{\phi_o}(\xi,\eta=l_o,\omega)$ is the projection $P_\phi(\xi)$ of $O(x,y)$ defined in Eq. (1) with $\phi_o = \phi + \frac{\pi}{2}$. Diffraction transmission tomography within the Rytov approximation thus reduces to conventional transmission tomography in the limit of vanishing wavelength. (See also [4-6].)

## 3. THE BACKPROPAGATION ALGORITHM

We conclude from the discussions presented in the first two sections that the reconstruction problem in transmission diffraction tomography within either the Born or Rytov approximations consists ultimately of solving the Fredholm integral equation (9) for $O(\underline{r})$ in terms of $D_{\phi_o}(\xi,\omega)$. Although, as discussed in the introduction, this equation can be approximately solved using Fourier synthesis, it is preferable to seek a direct solution in a form analogous to that provided by the filtered backprojection algorithm in conventional transmission computed tomography. In this section we shall derive such an algorithm which, for reasons which will become apparent from our discussion, we call the *filtered backpropagation algorithm.*

Consider the low pass filtered version of the profile $O(\underline{r})$ defined by

$$O_{LP}(\underline{r}) \equiv \frac{1}{(2\pi)^2}\int d^2K\, \tilde{O}_{LP}(\underline{K})e^{i\underline{K}\cdot\underline{r}} \quad , \tag{30}$$

where $\tilde{O}_{LP}(\underline{K}) = \tilde{O}(\underline{K})$ for $|\underline{K}| < \sqrt{2}k$ and is zero otherwise. Let us make the substitution $\underline{K} = k(\underline{s} - \underline{s}_o)$ in the integral in Eq. (30), where $\underline{s}_o = (\cos\phi_o, \sin\phi_o)$ and $\underline{s} = (\cos\chi, \sin\chi)$ are unit polar vectors whose azimuthal angles in the $K_x,K_y$ coordinate system are $\phi_o$ and $\chi$ , respectively. For this change of variables we then have[1]

$$K_x = k(\cos\chi - \cos\phi_o) \quad ,$$

$$K_y = k(\sin\chi - \sin\phi_o) \quad ,$$

$$dK_x dK_y = k^2\sqrt{1 - \cos^2(\chi-\phi_o)}\,d\chi d\phi_o$$

$$= k^2\sqrt{1 - (\underline{s}\cdot\underline{s}_o)^2}\,d\chi d\phi_o,$$

so that Eq. (30) becomes

$$O_{LP}(\underline{r}) = \frac{k^2}{2(2\pi)^2}\int_{-\pi}^{\pi}d\phi_o\int_{-\pi}^{\pi}d\chi\,\sqrt{1-(\underline{s}\cdot\underline{s}_o)^2}\tilde{O}_{LP}[k(\underline{s}-\underline{s}_o)]\,e^{ik(\underline{s}-\underline{s}_o)\cdot\underline{r}} \quad . \tag{31}$$

The factor of 1/2 appears in Eq. (31) because the integration over $2\pi$ radians in $\phi_o$ and $\chi$ results in double coverage of the region of integration $|\underline{K}| \leq \sqrt{2}k$.

The representation given in Eq. (31) is seen to be ideally suited for diffraction tomography since, for each $\phi_o$ , the integral over $\chi$ involves $\tilde{O}(\underline{K})$ evaluated on the locus of points defined in Eq. (10). The portion of the $\chi$ integral corresponding to values of $\underline{s}$ such that $\underline{s}\cdot\underline{s}_o > 0$ can then be evaluated entirely in terms of data (e.g., $\tilde{D}_{\phi_o}(\kappa,\omega)$ ) collected in an experiment employing an insonifying plane wave whose unit wavevector is $\underline{s}_o$ . We shall find below that the integrand of the $\chi$ integral vanishes when $\underline{s}\cdot\underline{s}_o < 0$ so that the entire integral can then be evaluated in terms of $\tilde{D}_{\phi_o}(\kappa,\omega)$.

To express $O_{LP}(\underline{r})$ in terms of $\tilde{D}_{\phi_o}(\kappa,\omega)$ we first note that Eq. (31) remains valid if we take $\chi$ to be the azimuthal angle of $\underline{s}$ relative to the $(\xi,\eta)$ coordinate system rather than the $K_x,K_y$ system (see Fig. 4). Relative to the $(\xi,\eta)$ coordinate system then

$$\cos\chi = \kappa/k \quad , \tag{32a}$$

$$\sin\chi = \frac{\sqrt{k^2-\kappa^2}}{k} \quad , \tag{32b}$$

with $-k \leq \kappa \leq k$. Note that the angle $\chi$ is restricted to lie in the interval $[0,\pi]$ . However, since $\tilde{O}_{LP}(\underline{K})$ vanishes for values of $|\underline{K}| \geq \sqrt{2}k$, $\tilde{O}_{LP}[k(\underline{s}-\underline{s}_o)]$ vanishes at all points lying on the circle corresponding to $\chi$ values lying in $[\pi,2\pi]$ and is equal to $\tilde{O}[k(\underline{s}-\underline{s}_o)]$ for $\chi$ lying in $[0,\pi]$. Upon making use of Eqs.(8), (9) and (32) we then find that the $\chi$ integral in Eq. (31) becomes

$$\int_0^{\pi}d\chi\,\sqrt{1-(\underline{s}\cdot\underline{s}_o)^2}\tilde{O}[k(\underline{s}-\underline{s}_o)]\,e^{ik(\underline{s}-\underline{s}_o)\cdot\underline{r}}$$

$$= \frac{1}{k}\int_{-k}^{k}\frac{d\kappa}{\gamma}|\kappa|\,\tilde{D}_{\phi_o}(\kappa,\omega)e^{i[\kappa\hat{\xi} + (\gamma - k)\underline{s}_o]\cdot\underline{r}} \quad , \tag{33}$$

where $\gamma = \sqrt{k^2 - \kappa^2}$ . Substituting Eq. (33) into Eq. (31) yields

$$O_{LP}(\underline{r}) = \frac{k}{2(2\pi)^2}\int_{-\pi}^{\pi}d\phi_o\int_{-k}^{k}\frac{d\kappa}{\gamma}|\kappa|\,\tilde{D}_{\phi_o}(\kappa,\omega)e^{i[\kappa\hat{\xi} + (\gamma - k)\underline{s}_o]\cdot\underline{r}} \quad . \tag{34}$$

Eq. (34) can be regarded as a generalization of Eq. (2) to the case of diffraction tomography. A slightly simplified result is obtained, however, if we express $\tilde{D}_{\phi_{\underline{s}}}(\kappa,\omega)$ in terms of the Fourier

[1]The author is indebted to Dr. S. Lang of Schlumberger-Doll Research and to one of the referees for suggesting the following derivation of Eq. (31). The original version of the paper contained a much less direct derivation that required a number of intermediate steps in passing from Eq. (30) to Eq. (31).

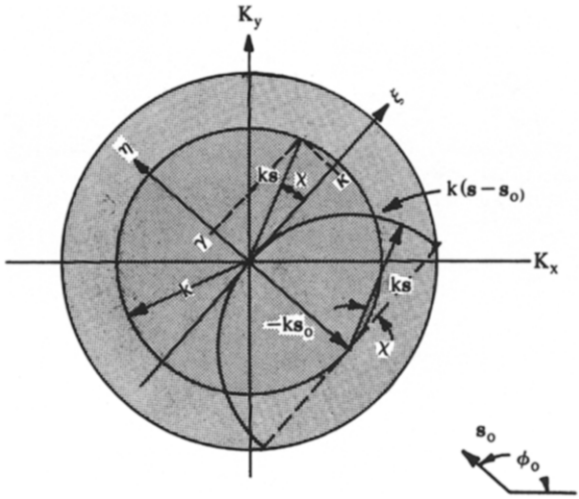


Fig. 4 Geometry used to evaluate the $\chi$ integral in Eq. (31). The quantity $\tilde{O}_{LP}(\underline{K})$ vanishes outside the shaded region so that $\chi$ need only range from 0 to $\pi$ in this integral.

transform of $\Gamma_{\phi_o}(\xi,\omega)$ defined in Eqs. (28) and (29) and note that $\underline{\xi}\cdot\underline{r} = \xi$ and $\underline{s}_o\cdot\underline{r} = \eta$, with $(\xi,\eta)$ being the coordinates of the point $\underline{r}$ in the $(\xi,\eta)$ coordinate system. We find that

$$O_{LP}(\underline{r}) = \frac{1}{(2\pi)^2}\int_{-\pi}^{\pi} d\phi_o \int_{-k}^{k} d\kappa |\kappa| \tilde{\Gamma}_{\phi_o}(\kappa,\omega) e^{i[\kappa\xi + (\gamma-k)(\eta-l_o)]} \quad , \tag{35}$$

where

$$\tilde{\Gamma}_{\phi_o}(\kappa,\omega) = \int_{-\infty}^{\infty} d\xi \Gamma_{\phi_o}(\xi,\omega) e^{-i\kappa\xi} \tag{36}$$

is the Fourier transform of $\Gamma_{\phi_o}(\xi,\omega)$.

The representation (35) can be employed to obtain reconstructions of $O_{LP}(\underline{r})$ much in the same way that the Fourier integral representation (2) can be employed in conventional transmission computed tomography. Alternatively, a reconstruction algorithm analogous to the filtered backprojection algorithm of conventional tomography can readily be derived from this representation. Toward this end we define the quantities

$$\hat{Q}_{\phi_o}(t) \equiv \int_{-\infty}^{\infty} \Gamma_{\phi_o}(\xi',\omega) h(t-\xi') d\xi' \quad , \tag{37}$$

where $h(t)$ is the filter function defined in Eq. (4) with $W = k$. The $\hat{Q}_{\phi_o}(t)$ are seen to be analogous to the filtered projections defined in Eq. (6). In terms of $\hat{Q}_{\phi_o}(t)$ we have, upon Fourier transforming Eq. (37),

$$\tilde{h}(\kappa)\tilde{\Gamma}_{\phi_o}(\kappa,\omega) = \int_{-\infty}^{\infty} dt' e^{-i\kappa t'} \hat{Q}_{\phi_o}(t') \quad , \tag{38}$$

where $\tilde{h}(\kappa) = |\kappa|$ for $|\kappa| \leq k$ and zero otherwise is the Fourier transform of $h(t)$. On substituting Eq. (38) into (35) we find that

$$O_{LP}(\underline{r}) = \frac{1}{(2\pi)^2}\int_{-\pi}^{\pi} d\phi_o \int_{k}^{k} d\kappa \left\{ \int_{-\infty}^{\infty} d\xi' e^{-i\kappa\xi'} \hat{Q}_{\phi_o}(\xi') \right\} e^{i[\kappa\xi + (\gamma-k)(\eta-l_o)]}$$

$$= \frac{1}{2\pi}\int_{-\pi}^{\pi} d\phi_o \int_{-\infty}^{\infty} d\xi' \hat{Q}_{\phi_o}(\xi') G(\xi-\xi',\eta-l_o) \quad , \tag{39}$$

where

$$G(\xi,\eta) \equiv \frac{1}{2\pi}\int_{-k}^{k} d\kappa e^{i[\kappa\xi + (\gamma-k)\eta]} \quad . \tag{40}$$

Finally, by defining the quantities

$$\Pi_{\phi_o}(\xi,\eta) \equiv \int_{-\infty}^{\infty} d\xi' \hat{Q}_{\phi_o}(\xi') G(\xi-\xi',\eta-l_o) \tag{41}$$

and putting $\xi = x\sin\phi_o - y\cos\phi_o$, $\eta = x\cos\phi_o + y\sin\phi_o$, we can write Eq. (39) in the final form

$$O_{LP}(\underline{r}) = \frac{1}{2\pi}\int_{-\pi}^{\pi} d\phi_o \Pi_{\phi_o}(x\sin\phi_o - y\cos\phi_o,\ x\cos\phi_o + y\sin\phi_o) \ . \tag{42}$$

We shall call the process of reconstructing $O_{LP}(\underline{r})$ via Eq. (42) the *filtered backpropagation algorithm.* This algorithm consists of first filtering the data $\Gamma_{\phi_o}(\xi',\omega)$ with the filter function $h(t)$. This step is identical to the filtering operation employed in conventional transmission computed tomography. Following the filtering operation the quantities $\Pi_{\phi_o}(\xi,\eta)$ must then be evaluated using Eq. (41) and, finally, superimposed according to Eq. (42) to yield $O_{LP}(\underline{r})$. We shall now show that the process of generating the $\Pi_{\phi_o}(\xi,\eta)$ from the $\hat{Q}_{\phi_o}(\xi)$ can be interpreted as a *backpropagation* into the half-space $\eta<l_o$ of the complex phase of a field propagating *into* the half-space $\eta>l_o$.

To show this consider the field $V(\underline{r}) = \exp[ik\eta + \Theta(\underline{r})]$ generated from sources to the inhomogeneous Helmholtz equation lying in the half-space $\eta<l_o$. It can be shown [21] that within the Rytov approximation $\Theta(\underline{r})$ propagates into the half-space $\eta>l_o$ according to the equation

$$\Theta(\underline{r}) = \frac{1}{2\pi}\int_{-\infty}^{\infty} d\kappa\ A(\kappa) e^{i[\kappa\xi + (\gamma-k)(\eta-l_o)]} \ , \tag{43}$$

with $\gamma = \sqrt{k^2-\kappa^2}$ and where $A(\kappa)$ is the one-dimensional Fourier transform of $\Theta(\underline{r})$ evaluated on the line $\eta=l_o$; i.e.,

$$A(\kappa) = \int_{-\infty}^{\infty} d\xi \Theta(\xi,\eta=l_o) e^{-i\kappa\xi} \ . \tag{44}$$

Now, for values of $|\kappa|$ exceeding $k = 2\pi/\lambda$, $\gamma$ is pure positive imaginary so that for such values of $\kappa$ the plane waves occuring in Eq. (43) decay exponentially when $\eta>l_o$. If we then neglect the contribution of these *evanescent* plane waves we obtain

$$\Theta(\underline{r}) \approx \frac{1}{2\pi}\int_{-k}^{k} d\kappa\ A(\kappa) e^{i[\kappa\xi + (\gamma-k)(\eta-l_o)]} = \int_{-\infty}^{\infty} d\xi' \Theta(\xi',\eta=l_o) G(\xi-\xi',\eta-l_o) \ , \tag{45}$$

with $G(\xi,\eta)$ defined in Eq. (40). We have then established the result that *in the absence of evanescent waves, the complex phase $\Theta(\underline{r})$ propagates, within the Rytov approximation, according to Eq. (45).*

The representation (45) allows one to determine the value of the phase $\Theta(\underline{r})$ at points $\xi,\eta$ lying in the half-space $\eta>l_o$ from the boundary value of this quantity on the line $\eta=l_o$. This process of determining a field quantity in a region *into which* the field is propagating from values of the quantity on the boundary of the region can be called *forward propagation.* Inverse propagation or *backpropagation* consists of the reverse process; i.e., determining a field quantity in a region *from which* the field is propagating from values of the quantity on the boundary of the region. As one might expect, backpropagation is much more difficult to achieve than forward propagation and, in general, can not be performed exactly due to information lost in the process of forward propagation [22]. However, it can be shown that if evanescent waves are neglected as is the case in Eq. (45), backpropagation is achieved via the same integral transform as forward propagation [22, 23]. Consequently, although Eq. (45) was originally derived for the process of forward propagation, it applies equally well to backpropagation. Of course this equation only approximates both processes since it holds only within the Rytov approximation and since evanescent waves were discarded in passing from Eq. (43) to Eq. (45).

We conclude from the discussion presented above that $\Pi_{\phi_o}(\xi,\eta)$, defined in Eq. (41), can be considered to be the backpropagated value of a complex phase whose boundary value on the line $\eta = l_o$ is $\hat{Q}_{\phi_o}(\xi)$. Referring to Eq. (37) we see that $\hat{Q}_{\phi_o}$ is linearly related to $\Gamma_{\phi_o}$ which, according to Eq. (29), is proportional to the complex phase function $\psi(\underline{r},\omega)$ of the field $U(\underline{r},\omega)$ generated by the interaction of the insonifying plane wave $\exp(ik\eta)$ with the object profile $O(\underline{r})$. (Note that this interpretation holds also within the Born approximation since, according to Eq. (19), $\exp(-ik\eta)U^{(s)}_{\phi_o}(\xi,\eta,\omega)$ propagates like a phase within the Born approximation. ) The $\Pi_{\phi_o}(\xi,\eta)$ can then be identified as being linear filtered versions of the backpropagated complex phase function of the field produced by the interaction of an insonifying plane wave with the object.

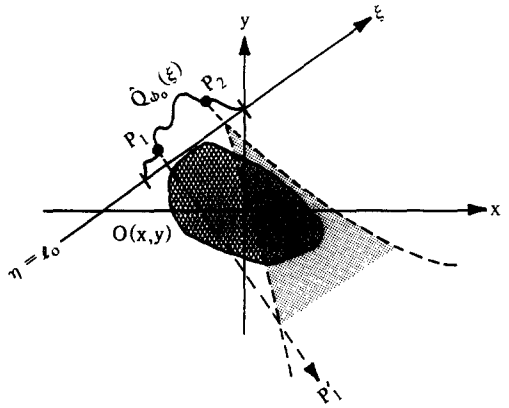


Fig. 5 Backprojection of $\hat{Q}_{\phi_0}(\xi)$ consists of assigning all points along the ray $P_1P'_1$ the value of $\hat{Q}_{\phi_0}(\xi)$ at $\xi=P_1$. In backpropagation the value of $\hat{Q}_{\phi_0}(\xi)$ at any given point such as $P_2$ produces the smeared out "image" $\hat{Q}_{\phi_0}(\xi=P_2)G(\xi-P_2, \eta-l_0)$ throughout the object space. In the short wavelength limit $G(\xi-P_2, \eta-l_0)$ reduces to the Dirac delta function $\delta(\xi-P_2)$ and backpropagation reduces to backprojection.

That the $\Pi_{\phi_0}$ should be backpropagated values of the filtered phase function of the field measured on the line $\eta = l_0$ is, in a certain sense, inevitable. Indeed, in diffraction transmission tomography the simple ray model employed in conventional transmission tomography is replaced by a model that incorporates wavelike features of the interaction process between the insonifying field and the object. It is only natural then that the backprojection operation of conventional tomography, which is a projection of a measured phase function back along straightline rays, should be replaced by *backpropagation,* a process by which a measured phase function is made to *propagate* back through the object space. Note that because backpropagation from the line $\eta = l_0$ is not the same as from the line $\eta = -l_0$, the integral in Eq. (42) is over $2\pi$ radians. Backprojection, on the other-hand, is reciprocal in this sense so that the integration in Eq. (5) is only over $\pi$ radians. The two operations backpropagation and backprojection are illustrated and compared in figure 5. The filtered backprojection and backpropagation algorithms are summarized in table 1.

Finally, we note that in the limit of vanishing wavelength the filtered backpropagation algorithm reduces, as it must, to the filtered backprojection algorithm of conventional transmission tomography. To show this we simply note that in the limit $k\to\infty$ ($\lambda\to 0$), $G(\xi,\eta)$ as defined in Eq. (40) tends to the Dirac delta function $\delta(\xi)$. Eq. (39) in this limit then yields the filtered backprojection algorithm of conventional transmission computed tomography.

## 4. THREE-DIMENSIONAL STRUCTURES

The results presented in the preceding sections apply to two-dimensional structures, i.e., objects whose properties vary only as a function of two in-plane coordinates such as, for example, the cartesian coordinates (x,y). In practice, of course, object profiles will vary in three dimensions so that O(x,y) must, in general, be replaced by O(x,y,z), with z being the third coordinate in the right-handed cartesian coordinate system (x,y,z). In this section we show how the filtered backpropagation algorithm derived in Section 3 can be applied to obtain *planar projections* of such three-dimensional structures. The complete three-dimensional profile can then be reconstructed from a sufficient number of such projections by making use of the projection-slice theorem [1].

The fundamental equations of diffraction tomography derived in Section 2 are easily generalized to three dimensions. In place of Eq. (20) one finds that over the *plane* $y = l_0$, the scattered field within the first Born approximation produced by an insonifying plane wave propagating along the y axis is [4-6]

$$U_B^{(s)}(x, y=l_0, z) = -i\frac{k^2}{8\pi^2}U_0(\omega)\int\int \frac{dK_x dK_z}{\gamma} e^{i\gamma l_0}\tilde{O}(K_x, \gamma-k, K_z)e^{i[K_x x + K_z z]}, \qquad (46)$$

where $\gamma = \sqrt{k^2-K_x^2-K_z^2}$. We find from Eq. (46) that the integral of $U_B^{(s)}(x, y=l_0, z)$ with respect to

TABLE 1. COMPARISON OF CONVENTIONAL AND DIFFRACTION TOMOGRAPHY.

| | | |
|---|---|---|
| **Data** | $\psi_{\phi_o}(\xi,\eta=l_o,\omega) = \frac{kU_o(\omega)}{2i}P_\phi(\xi)$ | $U^{(s)}_{\phi_o}(\xi,\eta=l_o,\omega) = \frac{kU_o(\omega)}{i}e^{ikl_o}\Gamma_{\phi_o}(\xi,\omega)$ ***Born*** <br> $\psi_{\phi_o}(\xi,\eta=l_o,\omega) = \frac{kU_o(\omega)}{i}\Gamma_{\phi_o}(\xi,\omega)$ ***Rytov*** |
| **Filter Operation** | $Q_\phi(t) = \int_{-\infty}^{\infty}d\xi' P_\phi(\xi')h(t-\xi')$ <br> $= \frac{2i}{kU_o(\omega)}\int_{-\infty}^{\infty}d\xi'\psi_{\phi_o}(\xi',\eta=l_o,\omega)h(t-\xi')$ | $\hat{Q}_{\phi_o}(t) = \int_{-\infty}^{\infty}d\xi'\Gamma_{\phi_o}(\xi',\omega)h(t-\xi')$ <br> $= \begin{cases} \frac{ie^{-ikl_o}}{kU_o(\omega)}\int_{-\infty}^{\infty}d\xi' U^{(s)}_{\phi_o}(\xi',\eta=l_o,\omega)h(t-\xi') & \textit{Born} \\ \frac{i}{kU_o(\omega)}\int_{-\infty}^{\infty}d\xi'\psi_{\phi_o}(\xi',\eta=l_o,\omega)h(t-\xi') & \textit{Rytov} \end{cases}$ |
| **Reconstruction** | ***Backprojection*** <br> $O(x,y) = \frac{1}{2\pi}\int_0^{\pi}d\phi Q_\phi(x\cos\phi + y\sin\phi)$ | ***Backpropagation*** <br> $\Pi_{\phi_o}(\xi,\eta) = \int_{-\infty}^{\infty}d\xi'\hat{Q}_{\phi_o}(\xi')G(\xi-\xi',\eta-l_o)$ <br> $O_{LP}(x,y) = \frac{1}{2\pi}\int_{-\pi}^{\pi}d\phi_o\,\Pi_{\phi_o}(x\sin\phi_o - y\cos\phi_o, x\cos\phi_o + y\sin\phi_o)$ |

the z coordinate is

$$\int_{-\infty}^{\infty}dz U_B^{(s)}(x,\ y=l_o,\ z) = -i\frac{k^2}{4\pi}U_o(\omega)\int\frac{dK_x}{\gamma}e^{i\gamma l_o}\tilde{O}(K_x,\ \gamma-k,\ 0)e^{iK_x x}\ , \tag{47}$$

with $\gamma = \sqrt{k^2-K_x^2}$. The right-hand side of Eq. (47) is seen to be identical to the right-hand side of Eq. (20) under the replacement of $\tilde{O}(K_x, \gamma-k)$ in Eq. (20) with $\tilde{O}(K_x, \gamma-k, 0)$. Moreover, upon performing a one-dimensional Fourier transform of Eq. (47) we obtain the result

$$\int_{-\infty}^{\infty}dz\int_{-\infty}^{\infty}dx\ U_B^{(s)}(x,\ y=l_o,\ z)e^{-i\kappa x} = -i\frac{k^2}{2}U_o(\omega)\frac{e^{i\gamma l_o}}{\gamma}\tilde{O}(\kappa,\ \gamma-k,\ 0)\ , \tag{48}$$

which is seen to be a three-dimensional counterpart of Eq. (23).

By substituting Eq. (46) into the three-dimensional version of Eq. (19) and essentially repeating the above analysis one obtains the following three-dimensional analog of Eq. (25):

$$\int_{-\infty}^{\infty}dz\int_{-\infty}^{\infty}dx\ \psi_R(x,\ y=l_o,\ z)e^{-i\kappa x} = -i\frac{k^2}{2}U_o(\omega)\frac{e^{i(\gamma-k)l_o}}{\gamma}\tilde{O}(\kappa,\ \gamma-k,\ 0)\ . \tag{49}$$

Just as in the two-dimensional case, Eqs. (48) and (49) can be generalized to the case of an insonifying plane wave propagating along an arbitrary $\eta$ axis such as illustrated in Figure 2. One then finds that in three dimensions one has, in place of Eqs. (9),

$$\tilde{D}_{\phi_o}(\kappa,\ \omega) = \int_{-\infty}^{\infty}d\xi D_{\phi_o}(\xi,\ \omega)e^{-i\kappa\xi} = \int\int dxdy\ O^P(x,y)e^{-ik(\underline{s}-\underline{s}_o)\cdot\underline{r}}\ , \tag{50}$$

where $D_{\phi_o}(\xi,\omega)$ is as defined in Eq. (28) with

$$\Gamma_{\phi_o}(\xi,\omega) = \begin{cases} \frac{ie^{-ikl_o}}{kU_o(\omega)}\int_{-\infty}^{\infty}d\alpha\ U^{(s)}_{\phi_o}(\xi,\eta=l_o,\alpha,\omega) & \text{Born Approximation} \quad (51a) \\ \frac{i}{kU_o(\omega)}\int_{-\infty}^{\infty}d\alpha\ \psi_{\phi_o}(\xi,\eta=l_o,\alpha,\omega) & \text{Rytov Approximation.} \quad (51b) \end{cases}$$

Here, $\alpha$ is the third cartesian coordinate in the right-handed $(\xi,\eta,\alpha)$ coordinate system and

$$O^P(x,y) = \int_{-\infty}^{\infty} dz\, O(x,y,z) \tag{52}$$

is the *planar projection* of $O(x,y,z)$ onto the plane $z = 0$.

The above equations are identical to the fundamental equations occuring in the two-dimensional case. All of the analysis and results presented in Section 3 then apply to three-dimensional structures; however, the *projection* $O^P(x,y)$ of the three-dimensional profile $O(x,y,z)$ takes the place of the two-dimensional profile $O(x,y)$. In particular, the filtered backpropagation algorithm Eq. (42) will apply in three dimensions yielding a low-pass filtered version $O^P_{LP}(x,y)$ of the planar projection $O^P(x,y)$.

To determine $O^P_{LP}(x,y)$ via the filtered backpropagation algorithm requires that many experiments be performed with the unit propagation vector $\underline{s}_o$ of the insonifying plane wave varying over the unit circle in the x-y plane. This amounts to keeping the measurement system fixed in space and rotating the object, assumed fixed relative to the (x,y,z) coordinate system, about the z axis. By rotating the object relative to the (x,y,z) coordinate system and then repeating the entire sequence of measurements one can then obtain a projection of the three-dimensional structure onto a different plane. By such a sequence of operations it is then possible to determine *any* planar projection of the object desired. Finally, the complete three-dimensional profile can be reconstructed from a sufficient number of such planar projections by making use of the three-dimensional projection-slice theorem [1].

## 5. SUMMARY

We have, in this paper, generalized the usual backprojection algorithm of parallel beam transmission computed tomography to be applicable to objects in which diffraction of the insonifying plane wave must be taken into account. The results apply to cases where the vector nature of the insonifying and scattered fields can be ignored (e.g., ultrasonic probing of biological media), and where the interaction between the field and object can be modeled via the first Born or Rytov approximations. For two-dimensional structures the derived algorithm yields directly the two-dimensional object profile while in three dimensions it yields planar projections of the profile from which the three-dimensional structure can be determined via the projection-slice theorem.

Various generalizations of the work reported here are possible. First and foremost it would be very desirable to derive a filtered backpropagation algorithm for *fan beam* geometries [2]. Since virtually all commercially available tomographic scanners use the fan beam geometry such a generalization seems essential. Other generalizations include developing an algorithm for cases where the vector nature of the fields must be taken into account. This is especially important in ultrasonic applications where shear waves can be introduced through mode conversion of insonifying compressional waves. Recent studies in inverse scattering [10] and diffraction tomography [24] have been devoted to this later case and it is hoped that by making use of the results of these and other studies [25] that the backpropagation algorithm derived here can be generalized to be applicable to tomography of elastic objects.

Certainly the most severe and serious limitation of the work presented here is the requirement that the field-object interaction be well modeled by the first Born or Rytov approximations. Unfortunately, it does not appear that viable solutions to two- and three-dimensional inverse scattering problems, such as diffraction tomography, can be obtained without imposing this restriction. Both the first Born and Rytov approximations yield *linear* relationships between the observed data and the object profile and therein lies the reason why a simple reconstruction algorithm such as that derived here is possible. Going beyond these approximations results in a formidable nonlinear problem (cf. [26]) for which, at present, no simple solution exists.

Finally, we mention that the filtered backpropagation algorithm has now been implemented and tested in computer simulations of diffraction tomography within the Rytov approximation [27]. The results of this study are extremely encouraging and indicate that the algorithm performs for diffraction tomography at least as well as does the filtered backprojection algorithm for conventional tomography. Work is currently in progress evaluating the algorithm in computer simulations of strongly refracting objects where the Rytov approximation is questionable and on data collected in actual ultrasonic experiments.

## REFERENCES


[1] Mersereau, R. M. and Oppenheim, A. V., Digital reconstruction of multidimensional signals from their projections, *Proc. IEEE 62*, 210-229 (1974).

[2] Kak, A. C., Computerized tomography with x-ray emission and ultrasound sources, *Proc. IEEE 67*, 1245-1272 (1979).

[3] Swindell, W. S. and Barrett, H. H., Computerized tomography: taking sectional x-rays, *Physics Today 30*, 32-41 (1977).

[4] Mueller, R. K., Kaveh, M., and Wade, G., Reconstructive tomography and applications to ultrasonics, *Proc. IEEE 67*, 567-587 (1979).

[5] Devaney, A. J., A New Approach to Emission and Transmission CT, in *1980 IEEE Ultrasonics Symposium Proceedings*, pp. 979-983 (IEEE Cat. No. 80CH 1602-2SU).

[6] Devaney, A. J., Inverse scattering theory within the Rytov approximation, *Opt. Lett. 6*, 374-376 (1981).

[7] Lipson, H. and Cochran, W., *The Determination of Crystal Structures* (Cornell University Press, Ithaca, NY, 1966).

[8] Vainshtein, B. K., *Diffraction of X-rays by Chain Molecules* (John Wiley, NY, 1974).

[9] Wolf, E., Three-dimensional structure determination of semi-transparent objects from holographic data, *Opt. Commun. 1*, 153-156 (1969).

[10] Norton, S. J. and Linzer, M., Ultrasonic reflectivity imaging in three dimensions: exact inverse scattering solutions for plane, cylindrical, and spherical apertures, *IEEE Trans. Biomed. Eng. BME-28*, 202-220 (1981).

[11] Carter, W. H., Computational reconstruction of scattering objects from holograms, *J. Opt. Soc. Am. 60*, 306-314 (1970).

[12] Mueller, R. K., Kaveh, M., and Inverson, R. D., A New Approach to Acoustic Tomography Using Diffraction Techniques, in *Acoustical Imaging Vol.8*, A. F. Metherell, ed., pp. 615-628 (Plenum Press, New York, 1980).

[13] Fercher, A. F., Bartelt, H., Becker, H., Wiltschko, E., Image formation by inversion of scattered field data: experiments and computational simulation, *Applied Optics 18*, 2427-2439 (1979).

[14] Devaney, A. J., Inverse Source and Scattering Problems in Optics, in *Optics in Four Dimensions*, Conference Proceedings 65, M. A. Machado and L. M. Narducci, eds., pp. 613-626 (Amer. Inst. Phys., New York, 1981).

[15] Stark, H. and Paul, I., An investigation of computerized tomography by direct Fourier inversion and optimum interpolation, *IEEE Trans. Biomed. Eng. BME-28*, 496-505 (1981).

[16] Greenleaf, J. F. and Bah, R. C., Clinical imaging with transmissive ultrasonic computerized tomography, *IEEE Trans. Biomed. Eng. BME-28*, 177-185 (1981).

[17] Tai, Chen-To, *Dyadic Green's Functions in Electromagnetic Theory*, Ch. 3 (In text Educ. Pub., Scranton, P.A., 1971).

[18] Tatarski, V. T., *Wave Propagation in a Turbulent Medium*, Ch. 7 (McGraw-Hill, New York, 1961).

[19] Chernov, L. A., *Wave Propagation in a Random Medium*, Ch. 5 (Dover Publications, Inc., New York, 1967).

[20] Morse, P. M. and Feshbach, H., *Methods of Theoretical Physics*, p. 823 (McGraw-Hill, New York, 1953).

[21] Devaney, A. J., Liff, H. J., and Apsell, S., Spectral representations for free space propagation of complex phase perturbations of optical fields, *Opt. Commun. 15*, 1-5 (1975).

[22] Shewell, J. R. and Wolf, E., Inverse diffraction and a new reciprocity theorem, *J. Opt. Soc. Am. 58*, 1596-1603 (1968).

[23] Sherman, G. C., Diffracted wave fields expressible by plane-wave expansions containing only homogeneous waves, *J. Opt. Soc. Am. 59*, 697-711 (1969).

[24] Mueller, R. K. and Kaveh, M., *Ultrasonic Diffraction Tomography*, Internal Rep. (Dept. Elec. Eng., Univ. Minnesota, MN).

[25] Gubernatis, J. E., Domany, E., Krumhansl, J. A., and Huberman, M., The Born approximation in the theory of scattering of elastic waves by flaws, *J. Appl. Phys. 48*, 2812-2819 (1977).

[26] Devaney, A. J. and Wolf, E., A new perturbation expansion for inverse scattering from three dimensional finite-range potentials, *Phys. Lett. 89A* , 269-272 (1982).

[27] Devaney, A. J., A computer simulation study of diffraction tomography, *IEEE Trans. Biomed. Eng.* (submitted).